

The Barkhausen Effect

Víctor Navas Portella

Facultat de Física, Universitat de Barcelona, Diagonal 645, 08028 Barcelona, Spain.

This work presents an introduction to the Barkhausen effect. First, experimental measurements of Barkhausen noise detected in a soft iron sample will be exposed and analysed. Two different kinds of simulations of the 2-d Out of Equilibrium Random Field Ising Model (RFIM) at $T=0$ will be performed in order to explain this effect: one with periodic boundary conditions (PBC) and the other with fixed boundary conditions (FBC). The first model represents a spin nucleation dynamics whereas the second one represents the dynamics of a single domain wall. Results from these two different models will be contrasted and discussed in order to understand the nature of this effect.

I. INTRODUCTION

The Barkhausen (BK) effect is a physical phenomenon which manifests during the magnetization process in ferromagnetic materials: an irregular noise appears in contrast with the external magnetic field \vec{H}_{ext} , which is varied smoothly with the time. This effect, discovered by the German physicist Heinrich Barkhausen in 1919, represents the first indirect evidence of the existence of magnetic domains. The discontinuities in this noise correspond to irregular fluctuations of domain walls whose motion proceeds in stochastic jumps or avalanches.

With the aim of measuring BK noise, experiments with a soft iron sample have been performed by using the method explained in section II. Experimental data have been collected and analysed. We focus our statistical analysis on BK noise data which are collected near the coercive field H_c , where the dominant magnetization mechanism is the motion of domain walls. Scale invariances and power law distributions of energies and amplitudes are found, which are typical features of critical phenomena.

The existence of disorder in the material is the main cause of BK effect. Among the different theories, the random field Ising model (RFIM) is a good way of explaining this effect through simulations. It must be said that this model does not consider surface effects neither the effect of demagnetizing fields. For these reasons, this model does not offer a proper explanation of a realistic material. However, since the goal is to extract statistical results from magnetization jumps (avalanches) in order to understand the critical behaviour of the system, this model will be used in simulations. It is important to remark that we consider the 2-d RFIM out of equilibrium. It displays a disorder-induced phase transition, which means that the parameter that controls the criticality of the system is the standard deviation (σ) associated to a Gaussian distribution of the local random fields.

In section III, some features of hysteresis processes in ferromagnetic materials are discussed in order to understand how BK noise appears. Two different versions of the 2-d non equilibrium RFIM at $T=0$ have been simulated with different boundary conditions which imply different behaviours of the system. Simulations of RFIM with Periodic Boundary Conditions (PBC) are repro-

duced and contrasted with other simulations from Ref.[1]. Moreover, a new version of RFIM with Fixed Boundary conditions (FBC) will be simulated in order to study a single domain wall which proceeds by avalanches. Differences between these two models will be explained in section IV.

II. EXPERIMENTS

BK experiments are based on the detection of the changes of magnetic flux in a secondary coil, which is fixed around the ferromagnetic sample, in response to a smooth change of an external field \vec{H}_{ext} produced by a primary coil. The change on the magnetic flux is given by:

$$\dot{\Phi} = A_{sc}\mu\vec{H}_{ext} + A_s\vec{I}, \quad (1)$$

where A_{sc} is the section of the secondary coil, which must be as small as possible in order to avoid demagnetizing fields effects, A_s is the section of the sample and I is its magnetization. The experimental setup is shown in Fig.1(a). All these components are placed inside a Faraday cage in order to reduce the external electromagnetic noise. A smoothly varying current is applied to the primary coil, while the change of magnetic flux in the secondary coil induces an electromotive force whose signal can be analysed by an oscilloscope or an A/D card after being suitably amplified. A signal is defined when the voltage exceeds from a fixed threshold and it finishes when the voltage remains below threshold during more than 200 μs . (See Fig.1(b)) In order to appreciate properly the BK noise, the optimal frequency of the applied voltage (triangular waveform) must be in the order of mHz (See Fig.1(c)). Near the coercive field $H_c (V \approx 0)$, where the dominant mechanism in the magnetization process is the domain wall motion, a large number of signals is detected (See Fig.1(d)). The signal obtained has to be considered as a sequence of elemental avalanches without superposition between them. In these conditions, a statistical analysis of the results can be done. By detecting every individual signal, the maximum value of the voltage V_{max} is used to obtain the signal amplitude

through the relation:

$$A = 20 \log \left(\frac{V_{max}}{1 \mu V} \right) - 40 (dB), \quad (2)$$

the energy associated to the signal can also be obtained by integrating the square of the detected voltage from the time t_i where the overflow voltage is detected until the signal has finished t_f following the criterion explained before.

$$E = \frac{1}{\Omega} \int_{t_i}^{t_f} |V(t)|^2 dt, \quad (3)$$

where $\Omega = 10k\Omega$ is the value of a reference resistance. Following this protocol, amplitude and energy distributions can be histogrammed (See Fig.1.(e).(f)). These distributions follow an approximate power law:

$$P(A) = A^{-\alpha} \quad (4)$$

$$P(E) = E^{-\epsilon} \quad (5)$$

It must be said that the experimental setup has a representative defect. The secondary coil is situated near the edge of the sample, outside the primary coil. If one tries to analyse the structure of BK activity can find difficulties due to the fact that, at the edges, it exists a non trivial configuration of magnetic domains. A solution to this problem could be to situate the secondary coil as far as possible from the edges of the sample, inside the primary coil.

III. MODELLING

A. Hysteresis processes in magnetic materials and magnetic domains model

Some energetic contributions are here exposed in order to understand macroscopic properties of the hysteresis loop and the BK noise from a microscopic point of view[2]. In a continuum approximation, the energy in a ferromagnetic material can be expressed as:

$$E = \sum_{\alpha=1}^3 \int d^3r \{ A(\vec{\nabla} M_{\alpha})^2 + k(M_{\alpha} e_{\alpha})^2 - (H_{\alpha}^{ext} + H_{\alpha}^d) H_{\alpha}^{ext} \} \quad (6)$$

where e_{α} are the components of easy-magnetization axis. The first term of this equation refers to the exchange energy, a short range interaction which tends to align the magnetic moments. The second term takes into account anisotropy, which tends to align magnetic moments with the easy magnetization axis. The last term is referred to the magnetic energy, which is caused by the interactions between magnetic moments and the external field \vec{H}^{ext} , which also includes the contribution of demagnetizing fields, which is a consequence of the surface boundaries.

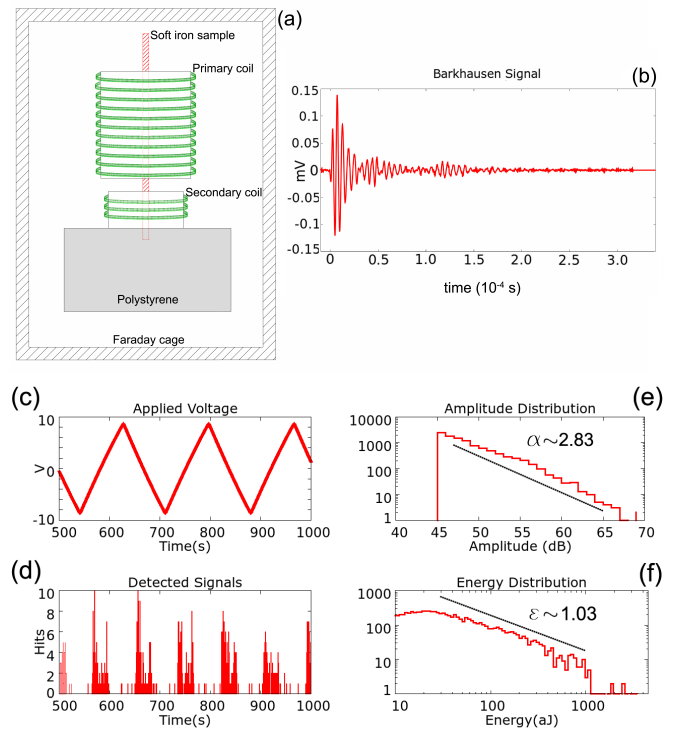


FIG. 1: Experimental setup and graphical results of the BK noise obtained from measurements using a soft iron sample. A single Barkhausen signal is shown in (b). Plot in (c) takes account of the applied voltage (20Vpp, triangular waveform) at a $f = 5mHz$. Plot in (d) represents the number of signals detected, where a 43dB threshold has been used to filter the values. Near a null applied voltage, which is interpreted as the coercive field, a large number of signals can be found. Plot in (e) represents the amplitude distribution while plot in (f) is a representation of the energy distribution. Exponents which fit in the amplitude and energy distributions are $\alpha = 2.83 \pm 0.08$ and $\epsilon = 1.03 \pm 0.03$.

The model described so far is useful to explain equilibrium situations. In equilibrium, the minimization of the energy in Eq.(6) explains the formation of magnetic domains. At $H^{ext} = 0$, an initially fully magnetized ferromagnetic system would split into magnetic domains in order to minimize the effect of demagnetizing fields. Hence the net magnetization would be zero (See Fig.2). Actually, this is not the case. Ferromagnetic alloys exhibit a net magnetization at zero external field (See Fig.3). Hysteresis can only be explained as a consequence of an out-of-equilibrium dynamics. A simple understanding can be obtained by a thermodynamic analysis. Below the critical temperature, if there is no external field applied, the free energy functional of a uni-axial ferromagnetic system can be represented as a double symmetric well in which the average magnetization is zero. When an external field is applied, the system tends to favour one of these wells, so this double well symmetry is broken. The free energy functional appears now as double asymmetric well, where the local minimum represents metastable

states and the global minimum represents stable states. The existence of a barrier between the two wells is what prevents the system relaxation. This free energy functional changes through a dynamical process dominated by the external field H^{ext} . The hysteresis loop has some

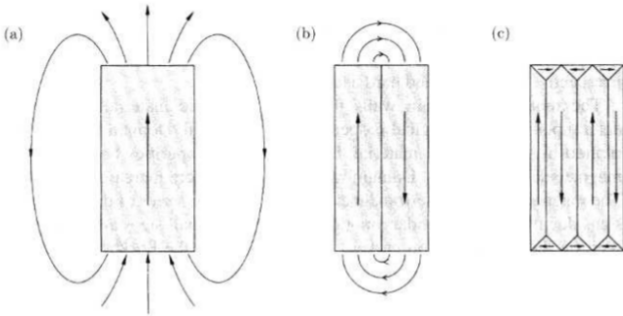


FIG. 2: Different domain walls configurations presents in a ferromagnetic material. Equilibrium situation ($H^{ext} = 0$) where the creation of magnetic domains reduces the effect of demagnetizing fields and leads to a null magnetization.[3]

representative features. The first characteristic is the fact that, at a given applied magnetic field, H_{sat} , the system is magnetized in one direction. At these points, the material possesses an unique magnetic domain and the system remains in a stable state: free energy global minimum. Another important characteristic is the presence of a net magnetization when the external magnetic field is zero, which is usually named as remanent magnetization M_r . This fact takes account of the collective phenomena characteristic of a ferromagnetic system. Another important feature of a hysteresis loop is the existence of magnetic field in which the magnetization is null: the coercive field H_c . In this sense, BK noise can be understood as the collective motion of domain walls along hysteresis loop. This collective motion of domain walls offers a change in magnetization which proceeds in small jumps or avalanches. (See Inset in Fig.3).

B. Spin model. Random Field Ising Model (RFIM)

From a general point of view, spin models consist of N interactive spins situated in the nodes of a d -dimensional lattice. The random field Ising model (RFIM) is a spin model where spins interact at nearest neighbours and can take the values $s_i = \pm 1$ ($i=1, \dots, N=L \times L$). In each node of the lattice, there is a random field h_i . The Hamiltonian reads:

$$\mathcal{H} = - \sum_{\langle ij \rangle} J s_i s_j - \sum_i (H + h_i) s_i \quad (7)$$

where, for simplicity, the exchange energy is considered as $J = 1$ and the local random fields $\{h_i\}$ follow a Gaus-

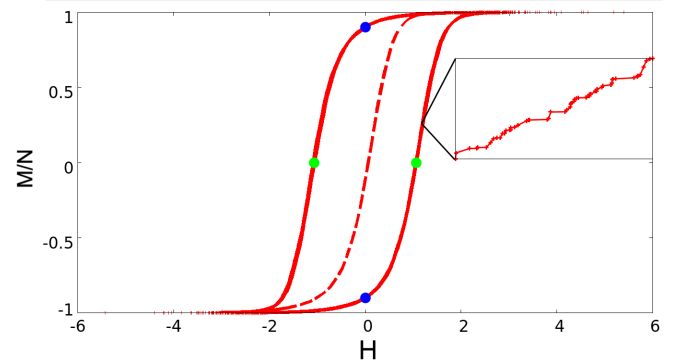


FIG. 3: Hysteresis loop single realization of the RFIM with periodic boundary conditions with a disorder parameter $\sigma = 2$. Blue points refer to the remanent magnetization M_r and green points refer to the coercive field H_c . Dashed line represents equilibrium situation. The inset plot shows how magnetization takes place in small jumps. These discontinuities in the magnetization process provoke the BK noise.

sian distribution:

$$\rho(h)dh = \frac{1}{\sqrt{2\pi\sigma^2}} \exp\left(-\frac{h^2}{2\sigma^2}\right) dh \quad (8)$$

Eq.(7) does not differentiate equilibrium from non-equilibrium states. In order to simulate metastable states, simulations have been driven as it follows. A spin will flip when its local field changes of sign.

$$h_i^{eff} = \sum_k s_k + H + h_i \quad (9)$$

This fact will change the local field of the immediate neighbours of the recent flipped spin. Depending on the sign of their local fields, any of these spins could be favourable to flip and the process continues in the same way generating an avalanche of flipping spins. The number of spins that have flipped in the same avalanche is considered as the size of the avalanche S . During each avalanche the external field is kept constant and, when there are no more unstable spins, which means that the system remains in a metastable equilibrium, the external field is increased again to generate a new avalanche. This is the so called adiabatic dynamics. Simulations are started with all the spins pointing down. Varying the external field, magnetization process takes place in form of avalanches until all the spins are pointing up. The algorithm that has been implemented is the 'brute force algorithm' described in Ref[4].

IV. RESULTS

A. Periodic Boundary Conditions (PBC)

Usually, RFIM is simulated with periodic boundary conditions. One then gets a spin nucleation dynamics. If

$\sigma < \sigma_c \sim 0.75$ an avalanche whose size is comparable to the dimensions of the system occurs generating, consequently, a sharp discontinuity in the magnetization (See Fig.4(a) and Fig.6(First row)). When $\sigma > \sigma_c$, the change of a spin is not so favourable to create a large avalanche and the magnetization evolves smoothly. (See Fig.4(b) and Fig.6(Second row)).

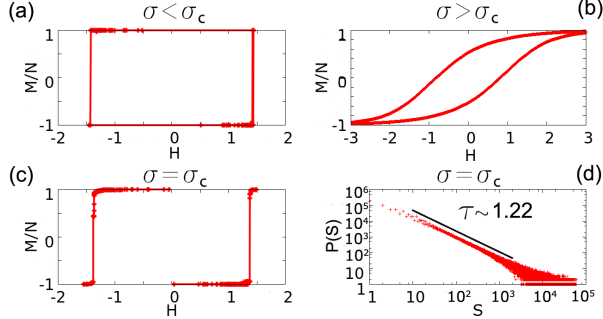


FIG. 4: Hysteresis loops simulated with the RFIM under periodic boundary conditions for N spins $N=L \times L$ ($L=256$) and different values of the disorder σ . Clearly, there is a disorder-induced phase transition for a certain value of σ_c . Below σ_c a big avalanche flips almost all the spins and over σ_c the magnetization process takes place in small avalanches. It is shown that, for σ_c the avalanche size distribution ($L=256, 10^3$ realizations) follows a power law.

In the thermodynamic limit, avalanches present a fractal nature at σ_c . Therefore, an analysis of the spanning avalanches (avalanches that span the whole system) has been carried out in order to determine an accurate value for σ_c . One expects to find a peak in the average number of spanning 1-d avalanches for σ_c similarly to what happens in percolation theory [5]. Focusing on this analysis, it has been found the value of the critical disorder, which depends on the dimensions of the system (See Fig.5(a)).

For the critical value of the disorder σ_c , the avalanche size distribution follows a power law whose exponent has a certain dependence with the dimensions of the system (See Fig.4(d)). The value of the exponent τ is $\tau = 1.22$ for $L=256$, $\tau = 1.25$ for $L=512$ and $\tau = 1.35$ for $L=1024$. All these fits have been done using a Maximum Likelihood method, which consists in adjusting a certain distribution function to empirical data[6].

In order to understand better all these models, phase diagrams have been plotted (See Fig.7(a)). These phase diagrams have to be understood out of equilibrium and at $T=0$. H_c is not the critical field but the coercive field. It is known that in 2-d, the critical field where the big avalanche takes place has the same value as the coercive field. One can see that, for small values of σ there is a tendency $H_c \rightarrow 4$. Analysing Eq.(9) for $\sigma \rightarrow 0$ ($h_i \rightarrow 0$) and focusing in a single spin, all the neighbours are pointing down, so the field that must be applied for small values of σ must be 4 in order to flip all the spins in the lattice.

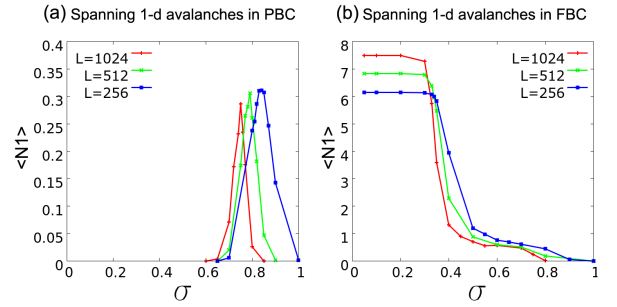


FIG. 5: Analysis of spanning 1-d avalanches for both models. All the values here presented have been averaged over 10^3 realizations, except some points near the peak of the smallest system ($L=256$) for PBC which have been averaged over 10^4 realizations. Straight lines, joining data sets, are guides to the eye. As it can be observed, for the PBC model three peaks are found at $\sigma_c = 0.84$ for $L=256$, $\sigma_c = 0.79$ for $L=512$ and $\sigma_c = 0.75$ for $L=1024$. Results for $L=1024$ have been checked and contrasted with Ref.[2] For the FBC a different structure can be appreciated.

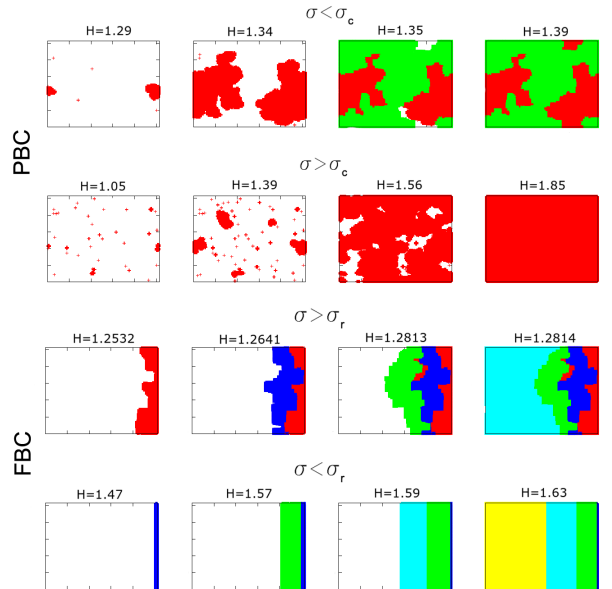


FIG. 6: Snapshots of configurations for $N=L \times L$ ($L=256$) in PBC and FBC models for different parameters of disorder σ . Red coloured spins correspond to non spanning avalanches (spins that have flipped from down to up). Avalanches of different color from red are spanning avalanches. First row is a system evolution with periodic boundary conditions for $\sigma = 0.75$, below σ_c . The second row corresponds to the same model with $\sigma = 0.9$, over σ_c . In these two plots can be appreciated the presence of spin nucleation in different parts of the system and, for a disorder below σ_c a big avalanche (green coloured) flips a lot of spins. The third row corresponds to the system evolution with fixed boundary conditions, $\sigma = 0.6$ (below σ_c) and the last one corresponds to the same kind of system but with $\sigma = 0.2$ ($\sigma < \sigma_r$).

B. Fixed Boundary Conditions (FBC)

A novel version of the RFIM is simulated with fixed boundary conditions along the x direction while the periodic boundary condition in y direction are not altered. Extremal spins of the system are pointing up (+1) at $x=L$, and pointing down (-1) at $x=0$. This second model can be understood as a single domain wall which, through a dynamical process, magnetizes the system by means of a certain number of avalanches. If one repeats study of the spanning 1-d avalanches for this model, some notorious differences can be appreciated. (See Fig.5(b)). In this case, there is a reminiscence of the peaks from the PBC model, so, it exists the same phase transition. But, for lower values of the disorder parameter σ , there is a step which gets flat at a certain value which depends on the dimensions of the system as $n_{Av} = \beta L_x^\gamma$, where $\gamma = 0.163 \pm 0.005$ and $\beta = 0.89 \pm 0.03$. This unexpected behaviour explains that for small values of σ , the system has a tendency to be magnetized by means of a sequence of a certain number of flat spanning avalanches n_{Av} instead of having a big avalanche which flips all the spins. We conjecture that all this casuistic is due to another disorder-induced phase transition at σ_r . For $\sigma > \sigma_r$, the interface is rough (See Fig.6(Third row)). For $\sigma < \sigma_r$ the roughness of the interface disappears and it becomes flat. (See Fig.6(Fourth row))

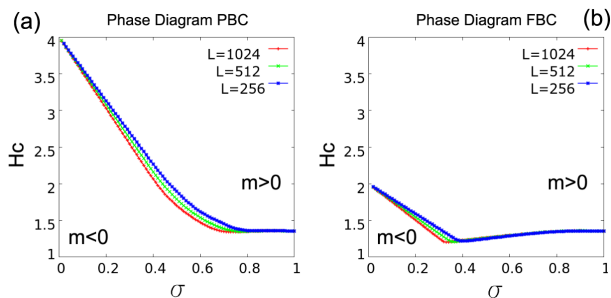


FIG. 7: Phase diagrams for the Fixed Boundary conditions model (FBC) and the Periodic Boundary conditions (PBC). For the FBC diagram it can be found the value of σ_r , which is $\sigma_r = 0.41$ for $L=256$, $\sigma_r = 0.36$ for $L=512$ and $\sigma_r = 0.34$ for $L=1024$. All points have been averaged over 10^2 realizations.

Observing the phase diagram for the FBC model, the system tends to $H_c \rightarrow 2$ when $\sigma \rightarrow 0$ (See Fig.7(b)). If Eq.(9) is analysed again $\sigma \rightarrow 0$ ($h_i \rightarrow 0$), one can observe

that, if there is a single interface, a spin situated at the boundary of the interface has three neighbours pointing down and one neighbour, corresponding to a flipped spin of the interface, pointing up. This configuration justifies that, in order to flip all the spins, the critical field needs to be 2. It should be noticed, that for large values of the disorder parameter σ , both models (PBC and FBC) have the same behaviour and the single interface has not a clear structure and spins flip through a nucleation process.

V. CONCLUSIONS

A description of hysteresis in ferromagnetic materials has been exposed. When disorder is present in the system, BK noise can be understood as a consequence of the domain wall motion which proceeds by means of jumps in magnetization, in response to a smoothly increasing external magnetic field. RFIM has been studied in order to offer a good description of the statistical features of the BK noise. In the two models presented (PBC and FBC), considering a range between $0.5 \sim \sigma \sim 1$, two different regions can be appreciated: one where the magnetization process takes place in small avalanches and another different region where a single avalanche, whose dimensions are comparable with the system, appears in the magnetization process. A new disorder-induced phase transition has been conjectured for the RFIM with FBC in which the rough interface becomes flat for a certain value of the disorder value σ . For $\sigma < \sigma_r$, the 2-d RFIM with fixed boundary conditions explains a magnetization process that takes place in a sequence of a finite number of flat spanning avalanches. The number of these avalanches has a certain dependence with the dimensions of the lattice. Concerning the comparison with experiments, there is no agreement between the exponent found for the amplitude distribution and the RFIM simulations.

Acknowledgements

I am grateful to Dr. E. Vives for his help and supervision of all the processes exposed in this work. I thank X.R.Hoffmann and N. Arredondo for some revisions and arrangements.

[1] D. Spasojević, S. Janičević and M. Knezević PHYSICAL REVIEW E 89, 012118 (2014)
 [2] G.Bertotti and I. Mayergoyz, 'The science of Hysteresis Vol.II.' 2005
 [3] S. Blundell "Magnetism in Condensed Matter", Oxford Univerity Press 2001

[4] M.C. Kuntz, O. Perkovic, K. A. Dahmen, B. W. Roberts and J- P. Sethna "Hysteresis, avalanches and noise"
 [5] I.D.Stauffer and A.Aharony "Introduction to percolation theory" Taylor and Francis, 1994
 [6] A.Clauset , C.R.Shalizi and M. E. J. Newman; " POWER-LAW DISTRIBUTIONS IN EMPIRICAL DATA" 2009